Inorganic Chemistry

ARTICLE

pubs.acs.org/IC

Modeling Structures and Vibrational Frequencies for Dinitrosyl Iron Complexes (DNICs) with Density Functional Theory

Scott M. Brothers,[†] Marcetta Y. Darensbourg,[†] and Michael B. Hall*[,†]

[†]Department of Chemistry, Texas A&M University, College Station, Texas 77840, United States

Supporting Information

ABSTRACT:

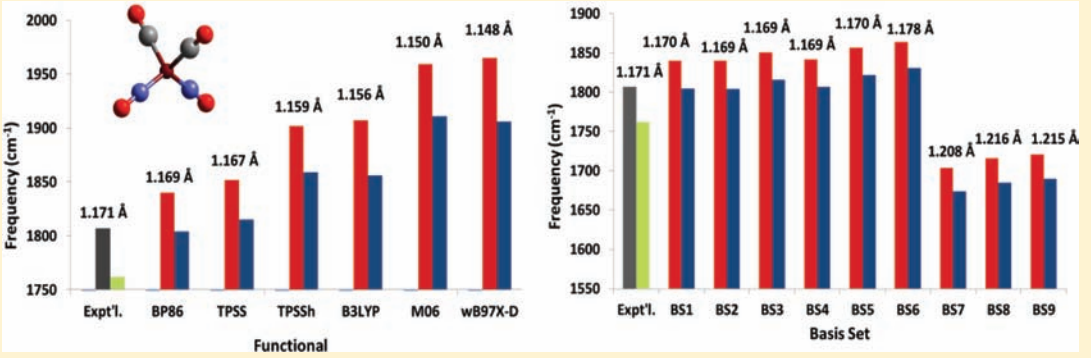

The biochemical and physiological importance of nitric oxide (NO) in signaling and vasodilation has been studied for several decades. The discovery of both protein-bound and free low molecular weight dinitrosyl iron complexes (DNICs) suggests that such compounds might play roles in biological NO storage and transport. These complexes have important distinguishing spectroscopic features, including EPR and Mössbauer spectra, and NO vibrational frequencies ($\nu_{(NO)}$). The latter are particularly sensitive to modifications of the ligand environment and metal oxidation states. Examinations of functionals and basis sets delineate their effect on the NO vibrational frequencies and allow development of a methodology to calculate these frequencies in other DNICs. Three complexes of the form $(L)(CO)Fe(NO)_2$ (L = CO, N,N′-dimethyl-imidazol-2-ylidene (IMe) or 1-methylimidazole (MeImid)), where $\{Fe(NO)_2\}^{10}$ is in its reduced form, have been used to calibrate the vibrational frequencies. The functional BP86 paired with a basis set of SDD/ECP on the metal and 6-311++G(d,p) on the ligand atoms exhibits the most accurate results, with deviations from experimental vibrational frequencies of no more than ± 40 cm^{-1}. Subsequent investigations were performed on a series of diiron trinitrosyl complexes of the form $\{Fe(NO)\}^7-\{Fe(NO)_2\}^9$ bridged by sulfurs, namely, $[(ON)Fe(\mu\text{-}S,S-C_6H_4)_2Fe(NO)_2]^-$, $[Fe(NO)_2\{Fe(NS_3)(NO)\}\text{-}\mu\text{-}S,S']$, and $[(ON)Fe(bme\text{-}dach)Fe(NO)_2\text{-}\mu\text{-}S,S']^+$, with the ideal functional/basis set pair determined via the aforementioned test set. The ground state energetics (singlet/triplet/singlet, respectively), geometric parameters, and nitrosyl vibrational frequencies were calculated. The results for the former two complexes correlated well with the experimental work, and in contrast with what was reported in an earlier computational study, a stable triplet ground state structure was optimized for $[Fe(NO)_2\{Fe(NS_3)(NO)\}\text{-}\mu\text{-}S,S']$. For $[(ON)Fe(bme\text{-}dach)Fe(NO)_2\text{-}\mu\text{-}S,S']^+$, whose synthesis and structure were recently reported, the geometric parameters, vibrational frequencies, and total energies compare well to experimental ones and favor a singlet ground state.

INTRODUCTION

Nitrosyl chemistry has been a topic of interest for chemists for several decades, as nitric oxide (NO), released from various reagents, can have beneficial pharmacological effects.[1] However, in excess, such as an atmospheric pollutant and with subsequent oxidation to NO_2, its deleterious nature is equally well-known.[2] Especially since 1990, enormous attention has been focused on the biological functions of NO such as signaling and neurotransmission,[3−5] vasodilation,[6] and immunology.[7,8] The discovery of NO bound to iron *in vivo* has led to a considerable body of work from inorganic chemists with the goal of modeling biological iron−nitrosyl complexes thereby mimicking the electronic structure and NO-release properties of these compounds.[9−13]

Biologically significant mononitrosyl iron complexes (MNICs) include the heme-based iron−nitrosyls as well as the as-isolated, inactive nitrile hydratase enzyme active site where the central Fe−NO occupies a tripeptide N_2S_2 coordination sphere.[14] Dinitrosyl iron complexes (DNICs) are known in high molecular weight forms where the $Fe(NO)_2$ units, resulting from iron−sulfur cluster degradation, are protein bound through cysteinyl

Received: May 27, 2011
Published: August 05, 2011

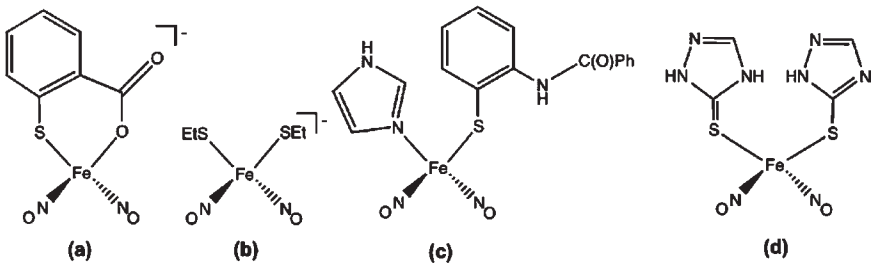

Figure 1. LMW-DNIC complexes containing thiolate, carboxylate, or imidazole donors.[11,15a]

sulfurs.[12] The corresponding low molecular weight dinitrosyl iron complexes (LMW-DNICs), released from the protein by free cysteine, histidine, or glutathione, are presumed to act as nitric oxide transport agents *in vivo*, while their protein bound precursors are expected to serve as NO storage units.[12] As an example, in the bis-cysteinyl $[(RS)_2Fe(NO)_2]^-$ species, the paramagnetic $[Fe(NO)_2]^+$ unit is described as the oxidized form of DNIC, and it is this form with its signature $g = 2.03$ EPR signal that has been targeted as a potential NO storage agent (in the high molecular weight (HMW), protein-bound form) and as a potential NO transport agent (in the LMW, protein-released form). Over the past decade, a number of biomimetic DNICs have been synthesized and fully characterized, particularly by Liaw and co-workers.[12] A small sample of synthetic LMW-DNIC complexes with biologically relevant thiolate, carboxylate, or imidazole ligands is shown in Figure 1.[11,15a] Additional instances of the $\{Fe(NO)_2\}$ motif are in the so-called "Roussin's red ester" complexes, which are a widely studied and well-characterized class of dimeric iron dinitrosyls bridged by sulfur atoms of the form $[(NO)_2Fe(\mu\text{-}SR)_2Fe(NO)_2]$.[13,15b,15c,16−21]

Transition metal nitrosyl complexes present challenging issues in the description and prediction of their electronic structure. The low-energy singly occupied π^* orbital of the NO ligand results in alternative assignments as NO^+, NO, and NO^- and correspondingly varying metal oxidation states. Enemark's and Feltham's (EF) notation $\{Fe(NO)\}^x$ avoids the oxidation state ambiguity by counting d and π^* electrons together as x.[22] For example, possible electronic configurations in the DNIC moiety of $L_2Fe(NO)_2$, where the spectator ligand L = a neutral two-electron donor ligand, may range from $[Fe^{2-}(NO^+)_2]$ to $[Fe^{2+}(NO^-)_2]$ with three intermediate combinations of Fe and NO redox levels between the two extremes. In the EF notation, these are all $\{Fe(NO)_2\}^{10}$. Although the EF notation avoids the oxidation state ambiguity, it hides the difficulty in describing and computing correctly the electronic structures that arise from the near degeneracy of the NO π^* and metal d orbitals.

To address the challenges of iron nitrosyl chemistry in both molecular and electronic structures, density functional theory proves to be a powerful tool to explain chemical phenomena that may be difficult to interpret via typical spectroscopic methods alone. As succinctly discussed by Neese, the selection of a particular functional can be vital depending on the parameters of interest. As an example, the pure functional BP86 has been known to provide accurate geometries and frequencies but to struggle with energetics, whereas PW91 is adept at calculation of the exchange couplings.[23] Although the standard functional in inorganic and bioinorganic chemistry has been B3LYP, which is fitted with chemically derived parameters,[24] more modern functionals without chemically derived parameters such as TPSS are also finding utility.[25] In short, although in many cases a routinely chosen functional/basis-set combination may perform reasonably well, in order to understand complicated series such as iron nitrosyl complexes, it is advisible to calibrate the functional and basis set via a test set of complexes.

While there are numerous DFT studies of mononitrosyl iron complexes (MNICs),[26] computational explorations of DNIC-type complexes remain sparse. Early studies of DNIC complexes sought to model their geometric properties, their spin densities, and parameters derived from Mössbauer spectroscopy.[26−29] Specifically, some of the most extensive computational investigations of nitrosyls have been performed by Ghosh and co-workers on structures of various iron nitrosyl composition.[26] Through this work, they determined that for iron nitrosyl complexes, the pure functional OLYP was a better compromise for geometric and electronic properties than the hybrid functional B3LYP.[26] Noodleman and co-workers performed broken-symmetry calculations on a series of mono-, bi-, and tetrametallic iron complexes with varying numbers of nitrosyl ligands bound to determine spin densities and oxidation states.[26c] Additionally, in work by Ye and Neese, isomer shifts, electronic characteristics, and molecular orbital diagrams of the DNIC $[(Ar\text{-}nacnac)Fe(NO)_2]$ in both its neutral $\{Fe(NO)_2\}^9$ and one-electron reduced $\{Fe(NO)_2\}^{10}$ forms were calculated and compared to experimental results.[27] However, to our knowledge, no comprehensive study has been performed on the important issue of modeling the nitrosyl infrared frequencies, which are characteristic of the electronic nature of the iron dinitrosyl unit and are important spectral signatures for both the EPR-active and EPR-silent states of DNICs.

In this work, we calculate the geometries and IR frequencies with various functionals and basis sets for a series of known monomeric $\{Fe(NO)_2\}^{10}$ complexes in order to determine the optimal pair. The methodology is then used to model two $\{Fe(NO)\}^7$−$\{Fe(NO)_2\}^9$ complexes previously investigated by Jaworska in order to compare our selected functional/basis set pair results for the ground state, IR frequencies, and geometries. We also explore the applicability of our methodology from the reduced $\{Fe(NO)_2\}^{10}$ complexes to oxidized $\{Fe(NO)_2\}^9$. To expand the computational work on $\{Fe(NO)\}^7$−$\{Fe(NO)_2\}^9$ complexes, we examine a newly synthesized complex, $[(NO)Fe(N_2S_2)Fe(NO)_2]^+$, where N_2S_2 = N,N′-bis(2-mercaptoethyl)-1,4-diazacycloheptane (bme-dach).[9]

COMPUTATIONAL DETAILS

Geometry and frequency calculations were performed at multiple levels of theory. Functionals utilized in this study included B3LYP,[30−32] BP86,[33,34] TPSS,[35] TPSSh,[35] M06,[36] and ωB97X-D.[37] The basis sets on the metal and ligand atoms were of a varying levels of complexity, and they are designated as follows:

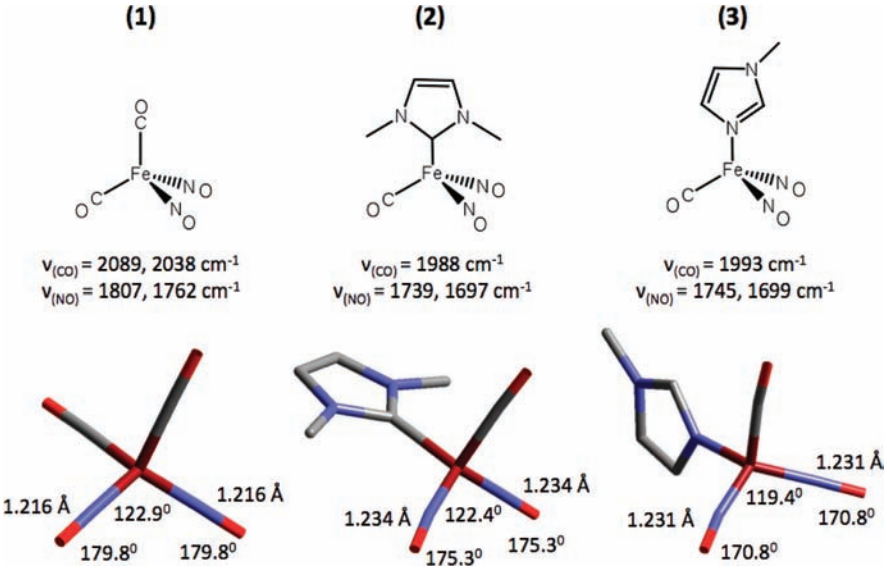

Figure 2. (L)(CO)Fe(NO)$_2$ series with salient geometric parameters and vibrational frequencies shown, where L = CO (**1**), IMe (N,N′-dimethylimidazol-2-ylidene) (**2**), and MeImid (1-methylimidazole) (**3**). [BP86/BS**2**].

(BS**1**) 6-311++G(d,p)
(BS**2**) Stuttgart-Dresden (SDD) effective core potential (ECP) on Fe,[38] 6-311++G(d,p) on light atoms (C,H,N, and O)
(BS**3**) SDD ECP on Fe, 6-311G(d,p) on light atoms
(BS**4**) 6-311++G on Fe, 6-311++G(d,p) on light atoms
(BS**5**) 6-311G(d,p)
(BS**6**) SDD ECP on Fe, 6-31G(d,p) on light atoms
(BS**7**) SDD ECP on Fe, 6-311G on light atoms
(BS**8**) SDD ECP on Fe, D95 (Dunning−Huzinaga full double-ζ) on light atoms
(BS**9**) LANL2DZ (Los Alamos National Laboratory 2-double-ζ) ECP on Fe,[39] D95 on light atoms

In complexes containing sulfur atoms, the double-ζ LANL2DZ ECP or all-electron triple-ζ basis sets were used with an additional *d* polarization function in the former case. These basis sets will be referred to as BS**X**$_{LANL}$ or BS**X**$_{POP}$.[40]

Where possible, input geometries were extracted from crystallographic coordinates and imported into *Ampac Graphical User Interface* (*AGUI*)[41] as starting geometries for the optimizations. For triplet species, the optimized singlet structure was used as the starting geometry. Geometry optimizations and frequency calculations were performed using the *Gaussian 09* software suite,[42] and the frequency calculations on stable geometries had no imaginary frequencies. Specifically, the frequency values were determined analytically via calculation of the second derivative of the energy by using the **Freq** keyword with default parameters in *Gaussian 09*. Selected complexes were analyzed with a solvation model using the polarizable continuum model (PCM) parameters for tetrahydrofuran as implemented in *Gaussian 09*. *AGUI* was used to extract the geometric properties and the infrared frequencies (including the vectors for stretching and bending) and to generate and render images of the frontier molecular orbitals. The 3D structures were drawn in *Cerius2*.[43] All energies in this manuscript have been converted from Hartrees to kilocalories per mole.

RESULTS AND DISCUSSION

Experimental Parameters of Complexes for Calibration. Three well-characterized DNICs, (L)(CO)Fe(NO)$_2$ (L = CO, IMe, and MeImid, see figure caption for ligand description), {Fe(NO)$_2$}^{10}, are displayed in Figure 2. For complex **1**, (CO)$_2$-Fe(NO)$_2$, the experimental infrared frequencies in tetrahydrofuran (THF) are $\nu_{(CO)}$ = 2089 and 2038 cm^{-1} and $\nu_{(NO)}$ = 1808 and 1762 cm^{-1}; from X-ray diffraction analysis, the average N−O bond distance is 1.171 Å.[44] The carbonyl ligands in complex **1** can be exchanged with ligands of varying donor strength with donor atoms being carbene−carbon, nitrogen, oxygen, sulfur, and phosphorus. Within the same redox level, exchanges with progressively stronger donor ligands lead to lower $\nu_{(CO)}$ and $\nu_{(NO)}$ values, as expected by classical π-back-bonding arguments.[45]

For this triad of complexes, we sought to examine several variables in the computational study: (1) functional, (2) diffuse and polarization functions, (3) the effect of triple- versus double-ζ basis sets on the metal, and (4) effect of triple- versus double-ζ basis sets on the ligand. The computational and experimental vibrational frequencies for complexes **1**−**3** can be compared in Table S1 (Supporting Information), and the salient geometric parameters of the experiment versus selected functional/basis set pairs for complexes **1** and **2** can be compared in Table S2 (Supporting Information). As of yet, no crystallographic data have been reported for complex **3**; only geometries of **1** and **2** are compared with theory.

Effect of Functionals on Vibrational Frequencies. For the six functionals investigated, three closely related pairs were found. The recently developed hybrid functionals M06 and ωB97X-D predicted the highest vibrational stretching frequencies, with the carbonyl frequencies calculated between 2000 and 2220 cm^{-1} and the nitrosyl frequencies between 1770 and 2000 cm^{-1} depending on the basis set. The traditional hybrid functionals B3LYP and TPSSh were similar to each other, with both carbonyl and nitrosyl values approximately 50−60 cm^{-1} lower than the values found for M06 and ωB97X-D. Finally, the nonhybrid functionals BP86 and TPSS were again similar to each other, with carbonyl and nitrosyl values approximately 50−100 cm^{-1} lower than B3LYP and TPSSh, respectively.

Effect of Diffuse and Polarization Functions on Vibrational Frequencies. The effect of the diffuse functions on the vibrational

frequencies can be determined by comparison (Table S1, Supporting Information) of BS**1**/BS**5** and BS**2**/BS**3** (diffuse/no diffuse functions). Removal of the diffuse functions from all atoms in the former and ligand atoms in the latter was probed. With the removal of diffuse functions on all atoms, the average difference in frequency between basis set pairs is approximately 10 cm^{-1} for CO stretching frequencies and approximately 20 cm^{-1} for NO stretching frequencies. In comparison, upon removal of the diffuse functions solely for the ligand atoms (BS**2** vs BS**3**), an average shift of the CO and NO frequencies is 5 cm^{-1} and 15 cm^{-1}, indicating a metal contribution of about 5 cm^{-1}, a relatively minor effect.

The effect of elimination of polarization functions on the ligands can be evaluated by comparing basis sets BS**3** (6-311G (d,p)) and BS**7** (6-311G). Loss of the light atom d orbital shifted the vibrational frequencies drastically, on the order of 130 to 150 cm^{-1} for both carbonyl and nitrosyl frequencies. Conversely, upon removal of the polarization functions on the metal (BS**1** vs BS**4**), no significant change in the calculated frequencies or bond distances is observed, indicating that the sensitivity of the frequencies to utilizing polarization functions lies predominantly on the ligand atoms rather than the metal center.

In order to determine whether the effect on polarization functions is intrinsic to the carbonyl and nitrosyl diatomic ligands or due to redistribution over the $\{Fe(NO)_2\}$ unit, the free ligands CO, NO^+, NO, and NO^- were calculated with basis sets BS**3** and BS**7** and with the functionals BP86, B3LYP, and ωB97x-D, and these results are presented below.

Intrinsic Properties of Diatomic Molecules CO and NO. To separate the effect of polarization functions on the carbonyls and nitrosyls of $(L)_2Fe(NO)_2$ complexes into an intrinsic effect on the diatomic ligands or an effect involving their interaction with the Fe in the $\{Fe(NO)_2\}$ unit, free CO as well as the three oxidation states of free NO (NO^+, NO, and NO^-) were calculated with BS**3** and BS**7** (polarization functions vs no polarization functions) with the three functionals BP86, B3LYP, and ωB97x-D. A table of these results can be found in the Supporting Information.

From this study, several important effects were realized:

(1) The hybrid functional B3LYP most accurately calculates the bond distances of the diatomic molecules with the basis set including polarization functions (BS**3**), with BP86 slightly overestimating and ωB97x-D slightly underestimating the bond distance. With no polarization functions, all bond distances were overestimated by at least 0.015 Å.

(2) However, BP86/BS**3** appears to be best for vibrational frequencies, with an error of -16 cm^{-1} for free CO and of -2 cm^{-1} for free NO. B3LYP calculates the frequencies to be roughly 100 cm^{-1} higher for both CO and NO, while ωB97x-D calculates them roughly 130$-$150 cm^{-1} higher, consistent with the results from the $(L)_2Fe(NO)_2$ complexes as described above.

(3) The difference in vibrational frequencies resulting from polarization functions appears to be intrinsic to the free diatomic molecules, as for the BP86 functional between basis sets BS**3** and BS**7**, the difference is approximately 150 cm^{-1} for CO and approximately 150$-$180 cm^{-1} for NO and NO^-, very similar to the effect of these functions in the $\{Fe(NO)_2\}$ complexes. Interestingly, the difference for NO^+ is much higher at approximately 250 cm^{-1}, a result consistent with the expected ligand character of NO to NO^- rather than NO^+.

Effect of Triple- Versus Double-ζ Basis Sets on Metal. The effect of the size of the basis set on the metal was examined by using two different basis sets with electron core potentials on iron, the triple-ζ SDD basis set[34] and the double-ζ LANL2DZ basis set, BS**8** and BS**9**.[35] The ligand basis set was minimized to the Dunning$-$Huzinaga full double-ζ (D95). These results are summarized in Table S1, Supporting Information. The difference between the two basis sets on the iron atom resulted in small differences in the CO frequencies (on average, $\sim$1$-$5 cm^{-1}) with a greater difference in the NO frequencies ($\sim$5$-$10 cm^{-1}), although the values are on par with or less than prior modifications, *vide supra*. Clearly, the nitrosyl frequencies were more sensitive in their response to changes in the iron basis set, affirming an effect, albeit minor, resulting from delocalization of electron density on the $\{Fe(NO)_2\}$ unit.

Effect of Triple- Versus Double-ζ Basis Sets on Ligand. In a similar fashion, changes due to the basis set of the ligands were queried systematically through comparisons of double- and triple-ζ basis sets. In these experiments, SDD ECP was used as the standard basis set for iron, with the various ligand basis sets. The basis sets selected for comparison were BS**3** (6-311G(d,p))/BS**6** (6-31G(d,p)) and BS**7** (6-311G)/BS**8** (D95). In accordance with a change from a larger (triple-ζ) to a smaller (double-ζ) basis set, the nitrosyl frequencies shift by 15 cm^{-1}, while the carbonyl frequencies shift less systematically (negligible for BS**3**/BS**5** and 25 cm^{-1} for BS**6**/BS**7**).

Overall Commentary on Methodology. With respect to the calculated nitrosyl stretching frequencies, the variables discussed above can be ranked in order of greatest to smallest possible effect.

1) *Polarization functions on the ligand (150 cm^{-1})*
2) *Functional (60$-$120 cm^{-1})*
3) *Basis set of ligand (triple vs double ζ; 15 cm^{-1}) and diffuse functions on ligand (15 cm^{-1})*
4) *Basis set of metal (triple vs double ζ; 5$-$10 cm^{-1})*
5) *Diffuse functions on metal (5 cm^{-1})*
6) *Polarization functions on metal (0$-$5 cm^{-1})*

An ideal functional/basis set pair should be that which provides a simultaneously close match to the experimental complex geometry and the carbonyl and nitrosyl vibrational frequencies, while the complexity of the functional and size of the basis set are balanced between suitable results and computational cost.

One consequence of this study indicates that the basis set on the ligand atoms has far more influence on diatomic ligand vibrational frequency values than does the iron basis set. As expected, the calculated frequencies and bond distances are related, as shown in Figure 3. Comparison of the various functionals shows that the best functional for the average $\nu_{(NO)}$ is BP86. In this figure, it can be seen that a majority of the functionals achieve similar differences between the symmetric and the antisymmetric stretches of the dinitrosyls. Somewhat surprisingly, the new functionals M06 and ωB97X-D, thought to circumvent issues and improve results relative to classic functionals, perform the worst of the selected functionals due to a systematic underestimation of backbonding, reflected in shorter N$-$O bond distances and higher $\nu_{(NO)}$ values. It is worthwhile to note that in Figure 4, where the BP86 functional is used to compare to experimental results by virtue of the eight basis sets, the best match is with BS**1** and BS**2**, with BS**2** somewhat lower in computational cost due to the ECP on the metal.

dx.doi.org/10.1021/ic201137t |*Inorg. Chem.* 2011, 50, 8532–8540

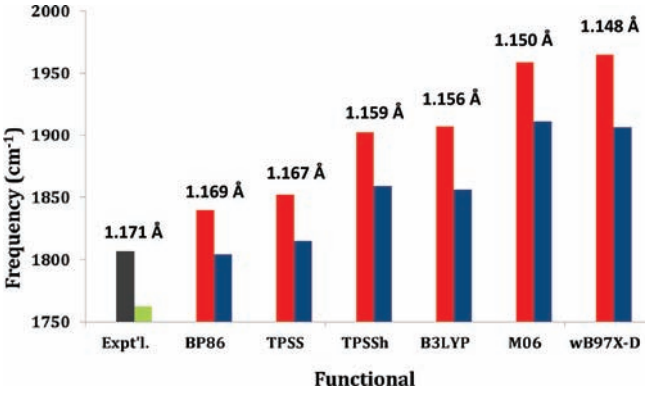

Figure 3. Frequency vs functional/experiment of $(CO)_2Fe(NO)_2$ using BS**2**. The average N−O bond distance is listed above the bars. The red bars represent the values for the symmetric stretch, and blue bars represent the antisymmetric stretch (gray and green bars are given for experimental values).

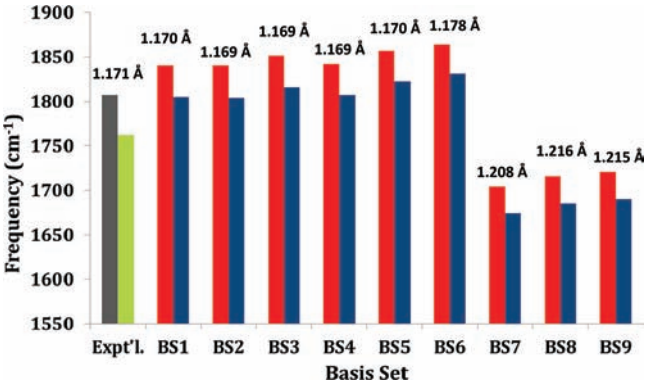

Figure 4. Frequency vs basis set/experiment of $(CO)_2Fe(NO)_2$ using BP86. The average N−O bond distance is listed above the bars. The red bars represent the values for the symmetric stretch, and blue bars represent the antisymmetric stretch (gray and green bars are given for experimental values).

Summarily, the best compromise between qualitative and quantitative results in both calculated vibrational stretching frequencies and N−O bond distances is found with BP86/BS**2** (although TPSS/BS**2** is quite similar). Interestingly, calculation of the vibrational frequencies using a PCM solvation model for THF at the BP86/BS**2** level of theory demonstrates a shift of both carbonyl frequencies (from 2049/2001 cm^{-1} in the gas phase to 2037/1973 cm^{-1} for **1**) and nitrosyl frequencies (from 1840/1804 cm^{-1} to 1809/1755 cm^{-1} for **1**), with a larger effect on the latter values. The Mulliken charges between the gas phase and solvation calculations can be compared in Table S3 (Supporting Information), indicating no significant charge redistribution. Due to these results, BP86 will be used further as the functional of choice.

COMPUTATIONAL INVESTIGATION OF $\{Fe(NO)\}^7$-$\{Fe(NO)_2\}^9$ COUPLED SYSTEMS

Commentary on the Experimental Properties of the $\{Fe(NO)\}^7$−$\{Fe(NO)_2\}^9$ Series. A series of $[(NO)Fe(L)Fe(NO)_2]^n$ (n = −1, 0, +1) complexes is shown in Figure 5, and we utilized our methodology to model these with BP86/BS**2** combinations. In this study, for all figures and tables, Fe′ refers to the mononitrosyl iron and Fe″ refers to the dinitrosyl iron.

Complex **4**, synthesized by Liaw and co-workers, was found to be diamagnetic.[46] Despite the similarities of the diamond-shaped Fe_2S_2 core of **4** and **5**, complex **5** demonstrates quite different vibrational frequencies, a longer Fe−Fe distance (2.669 Å for **4** vs 2.766 Å for **5**), and a magnetic moment of μ_{eff} = 2.81 μ_B, signifying a triplet ground state.[47] The geometric and spectroscopic properties are summarized in Table 1.

In previous computational investigations of **4** and **5**, the B3LYP/6-311G* functional/basis set pair (in our notation, B3LYP/BS**3**) was used to optimize the geometry and to determine the magnetic coupling,[28] and in a second study of complex **5**, broken-symmetry calculations were used to model the Mössbauer parameters.[26] Jaworska examined the natural orbitals of **4** and **5** and found antiferromagnetic coupling in the $[(NO)Fe(\mu\text{-}S)_2Fe(NO)_2]$ core in each case.[28]

Complex **6** has been recently synthesized in our laboratory. Rather than the diamond-shaped Fe_2S_2 core found in **4** and **5**, the complex adopts a butterfly-shaped core with an Fe−Fe distance of 2.786 Å.[7] This observed difference in geometry is likely related to the increase in the vibrational stretching frequencies of the dinitrosyl unit compared to those of **4** and **5**, with the mononitrosyl vibrational energy between that of the symmetric and antisymmetric stretch, see Table 1.

In an effort to integrate complex **6** with **4** and **5** as a related series and to serve as a test set for our methodology described above, we used the calibrated functional/basis sets (BP86/BS2_{LANL}; BP86/BS2_{POP}) to model the vibrational frequencies and optimized geometries of the bimetallics. Salient computational values are presented alongside the experimental in Table 1.

Computational Exploration of $[(NO)Fe(\mu\text{-}S)_2Fe(NO)_2]$ Complexes 4, 5, and 6. The crystallographic structures of complexes **4**, **5**, and **6** were utilized as the starting structures for the full optimizations at the BP86/BS2_{LANL} level of theory. Both the singlet and triplet state of this series of complexes were calculated, and in nearly all instances, the optimized geometry of the appropriate ground state structure matched reasonably well with the crystallographic parameters. One notable exception was in the triplet state of complex **5**. When optimized starting from the singlet geometry, the triplet optimized with a linear NO and large Fe−Fe distance in contrast to the experimental results. In a second optimization, the Fe′−N−O angle was initially frozen at the experimental value and the geometry allowed to relax. The new starting structure was fully optimized to a triplet-state geometry, which corresponds well to the crystallographic data. The three optimized structures are shown in Figure 5, and the geometric and vibrational frequency values can be compared in Table 1. The degree of coupling between the $\{Fe'(NO)\}^7$ and $\{Fe''(NO)_2\}^9$ units is illustrated in Figure 6 where the normal coordinates are shown. For each structure, the contribution of each oscillator is shown in both magnitude and direction.

Consistent with the experimental NMR data,[46] complex **4** was predicted to be a singlet, with the triplet state nearly 15 kcal/mol higher in energy. The vibrational frequencies for both $\mathbf{4}_{sing}$ and $\mathbf{4}_{trip}$ match extremely well with those of $\mathbf{4}_{exp}$. Likewise, the Fe′−N−O angle and N−O distance were relatively independent of these states. Thus, by any of these measurements, it was futile to identify the ground state. However, the predicted Fe′−Fe″ distance expands from 2.649 Å in the singlet to 3.003

dx.doi.org/10.1021/ic201137t |*Inorg. Chem.* 2011, 50, 8532–8540

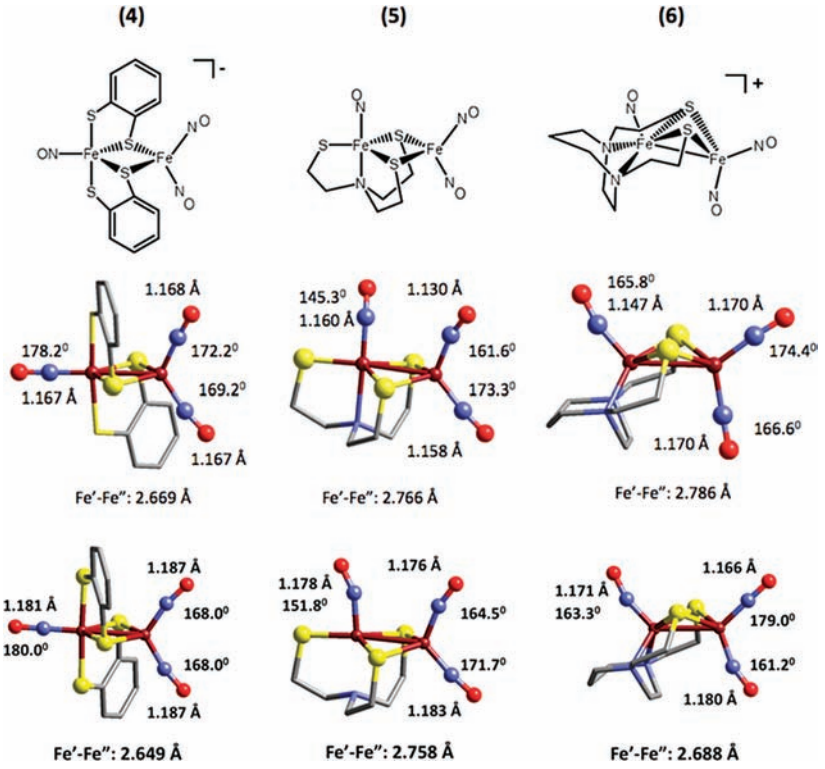

Figure 5. (From left to right) Experimental (top) and computational ground state (bottom) structures of $[(NO)Fe(S_4)Fe(NO)_2]^-$ (**4**),[46] $[(NO)Fe(NS_3)Fe(NO)_2]$ (**5**),[47] and $[(NO)Fe(N_2S_2)Fe(NO)_2]$ (**6**).[9] Fe′−Fe″ and N−O bond distances are given in addition to ∠Fe−N−O, and the $[(NO)Fe(\mu\text{-}S)_2Fe(NO)_2]$ core is represented as ball and stick drawings.

Å in the triplet, and the former corresponds well with the experiment. Additionally, the Fe−(μ-S) distances match extremely well in the singlet geometry but are overestimated by nearly 0.1−0.2 Å in the triplet, corresponding to an average error of approximately 5%.

Complex **5**, which has been recently investigated by both Jaworska[28] and Ghosh and co-workers,[26b,c] has been reoptimized with our parameters. Three distinct isomers were found on the potential energy surface as follows: singlet state with a linear Fe′−N−O, triplet state with a linear Fe′−N−O, and a triplet state with a bent Fe′−N−O, the last of which is consistent with the crystallographic structure. The ground state was found to be the bent Fe′NO triplet structure, with the linear triplet 4.42 kcal/mol and the linear singlet 7.52 kcal/mol higher in energy. The crystallographic structure was reported to possess disorder in the Fe′NO and Fe″NO nitrosyl oxygen atoms positioned *cisoid* to one another, with two Fe′−N−O angles extracted from the data at 145.3/151.8° and the Fe″−N−O angle at 170.1/173.3°. The difficulty in accurate refinement of M−N−O complexes with nitrogen and sulfur based ligand sets has been previously noted.[48] Interestingly, the calculated Fe′−N−O angle for BP86 matched identically with the latter experimental value. The Fe′−Fe″ distance was calculated to be 2.758 Å, close to the experimental value of 2.766 Å. Finally, the frequencies of the lowest energy structure were calculated to be 1797, 1751, and 1719 cm^{-1} with the experimental values reported at 1789, 1736, and 1654 cm^{-1}. Thus, the two higher energy stretches match reasonably well, with a larger error in the lowest energy stretch. The assignment of the vibrational stretches, though, is determined to be appropriate with the visualization of the infrared frequencies identifying the lowest energy stretch as Fe′−N−O, consistent with the results of Hughes and co-workers.[47] Other salient geometric values, as well as those utilizing an alternate functional (TPSS) or basis set ($BS2_{LANL}$), can be observed in Table 1.

Extension of Methodology to Complex 6. From its sharp NMR features, the butterfly-shaped complex **6** is proposed to exist as a ground-state singlet.[9] With respect to the nature of the trinitrosyl butterfly complex, we sought to use our computational methodology to identify the ground state. Like complex **4**, which indicated a clear preference for the singlet state, $\mathbf{6}_{trip}$ was calculated to be only 5.32 kcal/mol (BP86) higher than $\mathbf{6}_{sing}$. The experimental assignment of the infrared data of **6**, in which the highest and lowest nitrosyl stretching frequencies are assigned to the $\{Fe(NO)_2\}^9$ and the middle nitrosyl frequency is assigned to the $\{Fe(NO)\}^7$ is confirmed upon examination of the spectral pattern and visualization of the normal infrared coordinates in the theoretical calculation.

Despite the better match of both the N−O and Fe−S bond distances for $\mathbf{6}_{sing}$ than for $\mathbf{6}_{trip}$, the Fe′−Fe″ distance (exp. 2.786 Å) is calculated too short in the singlet case (2.688 Å) and too long in the triplet case (2.978 Å). To alleviate concerns that the butterfly-shaped Fe_2S_2 core was not calculated with the same degree of accuracy as the diamond-shaped complexes due to a poor basis set on sulfur, all complexes were recalculated using the all-electron 6-311++G(d,p) basis set on sulfur. The results are found in Table 1 and show no significant difference in the computational values, with experimental vs computational differences of the vibrational frequencies on the same magnitude of error relative to the test set, indicating that larger molecules, such as those containing sulfur atoms, do not reflect sensitivity to the effects listed above. Thus, we assign the ground state structure to be a diamagnetic singlet by virtue of energy, the vibrational

dx.doi.org/10.1021/ic201137t |*Inorg. Chem.* 2011, 50, 8532–8540

Table 1. Experimental and Computational Parameters for $\{Fe(NO)\}^7-\{Fe(NO)_2\}^9$ Complexes (Data in Italics Represent the Fe′NO Data)

	functional/basis set	total energy (kcal/mol)	$\nu_{(NO)}$ (cm^{-1})	Fe−N−O	N−O	Fe′−Fe″	Fe′−S	Fe′-(μ-S)	Fe″-(μ-S)
				$[(NO)Fe(S_4)Fe(NO)_2]^-$ (**4**)					
experimental			*1766*, 1746, 1719	172.2, 169.2, *178.2*	1.168, 1.167, *1.167*	2.669	2.293, 2.300	2.235, 2.247	2.286, 2.302
calculated ($S = 0$)	BP86/BS2$_{LANL}$	0	*1784*, 1759, 1724	168.0, 168.0, *180.0*	1.187, 1.187, *1.181*	2.649	2.335, 2.335	2.233, 2.233	2.307, 2.307
	BP86/BS2$_{POP}$	0	*1784*, 1758, 1723	167.7, 167.7, *180.0*	1.187, 1.187, *1.181*	2.656	2.334, 2.334	2.235, 2.235	2.307, 2.307
calculated ($S = 1$)	BP86/BS2$_{LANL}$	14.64	*1777*, 1740, 1726	167.9, 167.8, *175.2*	1.186, 1.186, *1.179*	3.003	2.355, 2.261	2.401, 2.320	2.340, 2.341
	BP86/BS2$_{POP}$	14.29	*1776*, 1738, 1724	167.8, 167.3, *174.9*	1.186, 1.186, *1.179*	3.011	2.352, 2.264	2.398, 2.319	2.340, 2.341
				$[(NO)Fe(NS_3)Fe(NO)_2]$ (**5**)					
experimental[a]			1789, 1736, *1654*	161.6, 173.3, *145.3*	1.130, 1.158, *1.160*	2.766	2.231	2.309, 2.355	2.298, 2.291
				170.1, 173.3, *151.8*	1.230, 1.158, *1.150*				
calculated ($S = 0$)	BP86/BS2$_{LANL}$	7.52	1829, 1777, *1739*	164.4, 174.1, *175.7*	1.179, 1.187, *1.171*	2.627	2.348	2.246, 2.232	2.265, 2.300
	BP86/BS2$_{POP}$	7.82	1831, 1776, *1738*	164.1, 174.0, *175.6*	1.179, 1.187, *1.170*	2.629	2.346	2.251, 2.234	2.269, 2.301
calculated ($S = 1$),	BP86/BS2$_{LANL}$	0	1797, 1751, *1719*	164.5, 171.7, *151.8*	1.176, 1.183, *1.178*	2.758	2.239	2.329, 2.365	2.296, 2.298
bent Fe^1NO	BP86/BS2$_{POP}$	0	1797, 1750, *1720*	164.4, 171.2, *151.9*	1.178, 1.183, *1.178*	2.765	2.241	2.329, 2.364	2.299, 2.300
				$[(NO)Fe(N_2S_2)Fe(NO)_2]$ (**6**)					
experimental			1795, *1763*, 1740	174.4, 166.6, *165.8*	1.170, 1.170, *1.147*	2.786		2.244, 2.259	2.252, 2.247
calculated ($S = 0$)	BP86/BS2$_{LANL}$	0	1849, *1803*, 1756	179.0, 161.2, *163.3*	1.166, 1.180, *1.171*	2.688		2.253, 2.253	2.236, 2.235
	BP86/BS2$_{POP}$	0	1849, *1803*, 1756	178.7, 161.0, *163.5*	1.166, 1.180, *1.171*	2.692		2.255, 2.255	2.238, 2.238
calculated ($S = 1$)	BP86/BS2$_{LANL}$	5.32	1839, *1780*, 1763	169.6, 169.4, *154.1*	1.166, 1.177, *1.172*	2.978		2.293, 2.293	2.319, 2.319
	BP86/BS2$_{POP}$	5.01	1838, *1779*, 1764	169.3, 168.9, *154.2*	1.166, 1.177, *1.172*	2.982		2.295, 2.295	2.321, 2.320

[a] The structure is reported to be disordered; both sets of data are shown.

dx.doi.org/10.1021/ic201137t |*Inorg. Chem.* 2011, 50, 8532–8540

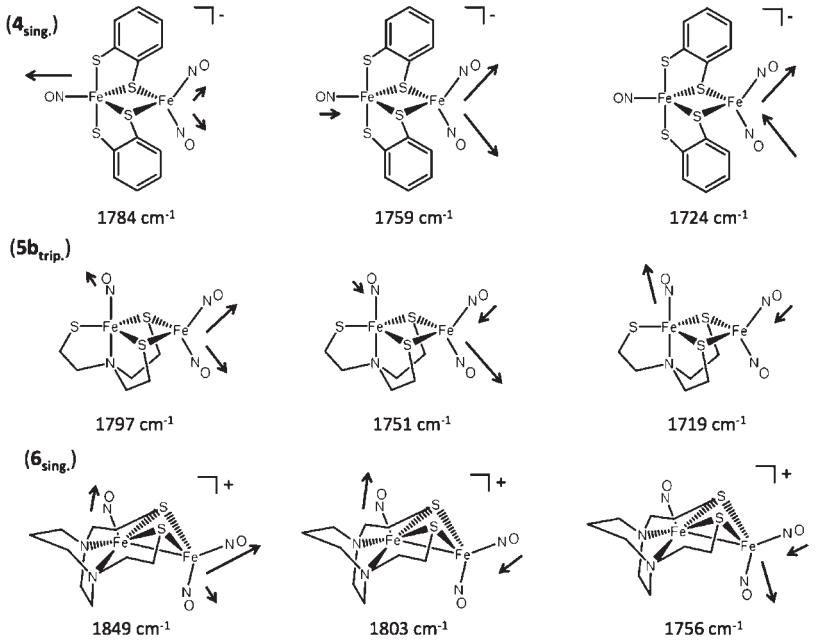

Figure 6. Vibrational coupling for the nitrosyl frequencies in the ground state structures of **4**, **5**, and **6**. Values listed correspond to BP86/BS**2**. The vibrational frequency represented is identified below the structures. The largest arrow represents the strongest nitrosyl stretch, and smaller stretches and contractions are represented by smaller arrows. The length of the arrows is roughly drawn to scale.

frequencies, and the correspondence of geometric parameters to those of experimental values.

SUMMARY AND COMMENTS

Examinations of various functionals and basis sets for the prediction of geometries and NO stretching frequencies in a series of $Fe(NO)_2$ complexes led to the following conclusions relative to the functional/basis set pairs. The $\nu_{(NO)}$ values are particularly sensitive to polarization functions on the ligands which are essential as their exclusion causes a positive shift of 150 cm^{-1} from the optimal calculated value. Less sensitive are diffuse functions on the ligand (15 cm^{-1}) or any significant changes to the metal (no shifts greater than 15 cm^{-1}). The functionals utilized in this work provide a range with a maximum difference of 120 cm^{-1}. In this manner, we discovered that the best compromise between basis set size, quality of results, and cost was BP86/BS**2** with TPSS/BS**2** a close second choice, whereas newer functionals such as M06 and ωB97x-D systematically underestimate the degree of backbonding, resulting in too short N−O bond distances and extremely high vibrational frequencies with better basis sets. Additionally, it is observed for the $(L)Fe(NO)_2(CO)$ complexes that NO is more sensitive to L both experimentally and theoretically than is CO, as a larger change in nitrosyl than carbonyl frequencies is seen for both the exchange of the ligand L and changes in the functional/basis set.

By utilizing our methodology, three known complexes containing a $\{Fe'(NO)\}^7-\{Fe''(NO)_2\}^9$ unit with a Fe_2S_2 bridging moiety and disparate geometries on the $\{Fe'(NO)\}^7$ fragment were calculated. Our computations confirmed that complex **4** is a singlet and complex **5** is a triplet, as has been concluded from experimental results. There was improved computational agreement in the case of complex **5**. Utilizing our methodology, we were able to mimic both the values of the frequencies as well as the assignments of the experimental stretches, with an extension to the newly synthesized complex **6**, which was calculated to have a singlet ground state with a low energy triplet state. This methodology is expected to have general utility for other $\{Fe(NO)_2\}$ applications.

ASSOCIATED CONTENT

Supporting Information. Tables of vibrational frequencies of **1**−**3**, a comparison of experimental and calculated geometric parameters of **1** and **2**, Mulliken charges of selected functional/basis set pairs, figures for $\mathbf{4}_{sing}$ and $\mathbf{4}_{trip}$, optimized coordinates for **1**−**6**, and representative input files for **1** and **4**. This information is available free of charge via the Internet at http://pubs.acs.org.

AUTHOR INFORMATION

Corresponding Author
*E-mail: hall@science.tamu.edu.

ACKNOWLEDGMENT

The authors appreciate support from the National Science Foundation (CHE-0910552 to MBH and CHE-0910679 to MYD) and the R.A. Welch Foundation (A-0648 to MBH and A-0924 to MYD). We further thank the National Science Foundation for continued support of our supercomputing facilities (CHE-0541587).

REFERENCES

(1) Lippard, S. J.; Berg, J. M. *Principles of Bioinorganic Chemistry*; University Science Books: Mill Valley, CA, 1994.

(2) Fontijn, A.; Sabadell, A. J.; Ronco, R. J. *Anal. Chem.* **1970**, *42*, 575.

(3) Rand, M. J.; Li, C. G.; La, M.; De Luca, A.; Najbar-Kaszkiel, A.; Jiang, F.; Di Iulio, J.; Ellis, A. *Asia Pac. J. Pharmacol.* **1997**, *12*, 137.
(4) Talman, W. T. *Ann. N.Y. Acad. Sci.* **1997**, *835*, 225.
(5) Lowenstein, C. J.; Dinerman, J. L.; Snyder, S. H. *Ann. Intern. Med.* **1994**, *120*, 227.
(6) Gladwin, M. T.; Raat, N. J. H.; Shiva, S.; Dezfulian, C.; Hogg, N.; Kim-Shapiro, D. B.; Patel, R. P. *Am. J. Physiol.* **2006**, *291*, H2026.
(7) Nahrevanian, H.; Amini, M. *Iran. J. Basic Med. Sci.* **2009**, *11*, 197.
(8) Tripathi, P. *Indian J. Biochem. Biophys.* **2007**, *44*, 310.
(9) Hsieh, C.-H.; Darensbourg, M. Y. *J. Am. Chem. Soc.* **2010**, *132*, 14118.
(10) Vanin, A. F.; Mikoyan, V. D.; Kubrina, L. N. *Biophysics* **2010**, *55*, 5.
(11) Chang, H.-H.; Huang, H.-J.; Ho, Y.-L.; Wen, Y.-D.; Huang, W.-N.; Chiou, S.-J. *Dalton Trans.* **2009**, 6396.
(12) (a) Chen, Y.-J.; Ku, W.-C.; Feng, L.-T.; Tsai, M.-L.; Hsieh, C.-H.; Hsu, W.-H.; Liaw, W.-F.; Hung, C.-H.; Chen, Y.-J. *J. Am. Chem. Soc.* **2008**, *130*, 10929. (b) Tsai, M.-L.; Hsieh, C.-H.; Liaw, W.-F. *Inorg. Chem.* **2007**, *46*, 5110. (c) Lu, T.-T.; Chiou, S.-J.; Chen, C.-Y.; Liaw, W.-F. *Inorg. Chem.* **2006**, *45*, 8799. (d) Tsai, M.-L.; Liaw, W.-F. *Inorg. Chem.* **2006**, *45*, 6583.
(13) Dillinger, S. A. T.; Schmalle, H. W.; Fox, T.; Berke, H. *Dalton Trans.* **2007**, 3562.
(14) Xu, N.; Yi, J.; Richter-Addo, G. B. *Inorg. Chem.* **2010**, *49*, 6253 and references therein.
(15) (a) Sanina, N. A.; Rakova, O. A.; Aldoshin, S. M.; Shilov, G. V.; Shul'ga, Y. M.; Kulikov, A. V.; Ovanesyan, N. S. *Mendeleev Commun.* **2004**, 7. (b) Rakova, O. A.; Sanina, N. A.; Shilov, G. V.; Shul'ga, Y. M.; Martynenko, V. M.; Ovanesyan, N. S.; Aldoshin, S. M. *Russ. J. Coord. Chem.* **2002**, *28*, 341. (c) Sanina, N. A.; Rakova, O. A.; Aldoshin, S. M.; Chuev, I. I.; Atovmyan, E. G.; Ovanesyan, N. S. *Russ. J. Coord. Chem.* **2001**, *27*, 179.
(16) Glidewell, C.; Harman, M. E.; Hursthouse, M. B.; Johnson, I. L.; Motevalli, M. *J. Chem. Res.* **1988**, *212*, 1676.
(17) Marsh, R. E.; Spek, A. L. *Acta Crystallogr.* **2001**, *57*, 800.
(18) Harrop, T. C.; Song, D.; Lippard, S. J. *J. Inorg. Biochem.* **2007**, *101*, 1730.
(19) Harrop, T. C.; Song, D.; Lippard, S. J. *J. Am. Chem. Soc.* **2006**, *128*, 3528.
(20) (a) Chen, Y.-J.; Ku, W.-C.; Feng, L.-T.; Tsai, M.-L.; Hsieh, C.-H.; Hsu, W.-H.; Liaw, W.-F.; Hung, C.-H.; Chen, Y.-J. *J. Am. Chem. Soc.* **2008**, *130*, 10929. (b) Lu, T.-T.; Tsou, C.-C.; Huang, H.-W.; Hsu, I.-J.; Chen, J.-M.; Kuo, T.-S.; Wang, Y.; Liaw, W.-F. *Inorg. Chem.* **2008**, *47*, 6040. (c) Tsou, C.-C.; Lu, T.-T.; Liaw, W.-F. *J. Am. Chem. Soc.* **2007**, *129*, 12626.
(21) Wang, R.; Camacho-Fernandez, M. A.; Xu, W.; Zhang, J.; Li, L. *Dalton Trans* **2009**, 777.
(22) Enemark, J. H.; Feltham, R. D. *Coord. Chem. Rev.* **1974**, *13*, 339. In this notation, the number of d electrons on the metal is summed with the π^* electrons of the nitrosyl. For example, an $\{Fe^{II}NO^{\bullet}\}$ system (which can be expressed as $\{Fe^{I}NO^{+}\}$ or $\{Fe^{III}NO^{-}\}$ as well) would have six d electrons and one π^* electron, making it a $\{FeNO\}^7$ system.
(23) Neese, F. *Coord. Chem. Rev.* **2009**, *253*, 526.
(24) Cramer, C. J. *Essentials of Computational Chemistry*, 2nd ed.; Wiley: West Sussex, England, 2004.
(25) Perdew, J. P.; Ruzsinszky, A.; Tao, J.; Staroverov, V. N.; Scuseria, G. E.; Csonka, G. I. *J. Chem. Phys.* **2005**, *123*, 062201.
(26) (a) Conradie, J.; Hopmann, K. H.; Ghosh, A. *J. Phys. Chem. B* **2010**, *114*, 8517. (b) Hopmann, K. H.; Noodleman, L.; Ghosh, A. *Chem.—Eur. J.* **2010**, *16*, 10397. (c) Hopmann, K. H.; Ghosh, A.; Noodleman, L. *Inorg. Chem.* **2009**, *48*, 9155. (d) Hopmann, K. H.; Conradie, J.; Ghosh, A. *J. Phys. Chem. B* **2009**, *113*, 10540.
(27) Ye, S.; Neese, F. *J. Am. Chem. Soc.* **2010**, *132*, 3646.
(28) Jaworska, M. *Polyhedron* **2007**, *26*, 3247.
(29) Shestakov, A. F.; Shul'ga, Y. M.; Emel'yanova, N. S.; Sanina, N. A.; Aldoshin, S. M. *Russ. Chem. Bull., Int. Ed.* **2007**, *56*, 1289.
(30) Becke, A. D. *J. Chem. Phys.* **1993**, *98*, 5648.
(31) Lee, C.; Yang, W.; Parr, R. G. *Phys. Rev. B: Condens. Matter Mater. Phys.* **1988**, *37*, 785.
(32) Miehlich, B.; Savin, A.; Stoll, H.; Preuss, H. *Chem. Phys. Lett.* **1989**, *157*, 200.
(33) Becke, A. D. *Phys. Rev. A: At., Mol., Opt. Phys.* **1988**, *38*, 3098.
(34) Perdew, J. P. *Phys. Rev. B: Condens. Matter Mater. Phys.* **1986**, *33*, 8822–8824.
(35) Tao, J. M.; Perdew, J. P.; Staroverov, V. N.; Scuseria, G. E. *Phys. Rev. Lett.* **2003**, *91*, 146401.
(36) Zhao, Y.; Truhlar, D. G. *Theor. Chem. Acc.* **2008**, *120*, 215.
(37) Hay, P. J.; Wadt, W. R. *J. Chem. Phys.* **1985**, *82*, 270.
(38) Chai, J.-D.; Head-Gordon, M. *Phys. Chem. Chem. Phys.* **2008**, *10*, 6615.
(39) Kaupp, M.; Schleyer, P. V. R.; Stoll, H.; Preuss, H. *J. Chem. Phys.* **1991**, *94*, 1360.
(40) Check, C. E.; Faust, T. O.; Bailey, J. M.; Wright, B. J.; Gilbert, T. M.; Sunderlin, L. S. *J. Phys. Chem. A.* **2001**, *105*, 8111.
(41) *AMPAC 9*; Semichem, Inc.: Shawnee, KS, 1992−2008.
(42) Frisch, M. J.; Trucks, G. W.; Schlegel, H. B.; Scuseria, G. E.; Robb, M. A.; Cheeseman, J. R.; Scalmani, G.; Barone, V.; Mennucci, B.; Petersson, G. A.; Nakatsuji, H.; Caricato, M.; Li, X.; Hratchian, H. P.; Izmaylov, A. F.; Bloino, J.; Zheng, G.; Sonnenberg, J. L.; Hada, M.; Ehara, M.; Toyota, K.; Fukuda, R.; Hasegawa, J.; Ishida, M.; Nakajima, T.; Honda, Y.; Kitao, O.; Nakai, H.; Vreven, T.; Montgomery, J. A., Jr.; Peralta, J. E.; Ogliaro, F.; Bearpark, M.; Heyd, J. J.; Brothers, E.; Kudin, K. N.; Staroverov, V. N.; Kobayashi, R.; Normand, J.; Raghavachari, K.; Rendell, A.; Burant, J. C.; Iyengar, S. S.; Tomasi, J.; Cossi, M.; Rega, N.; Millam, N. J.; Klene, M.; Knox, J. E.; Cross, J. B.; Bakken, V.; Adamo, C.; Jaramillo, J.; Gomperts, R.; Stratmann, R. E.; Yazyev, O.; Austin, A. J.; Cammi, R.; Pomelli, C.; Ochterski, J. W.; Martin, R. L.; Morokuma, K.; Zakrzewski, V. G.; Voth, G. A.; Salvador, P.; Dannenberg, J. J.; Dapprich, S.; Daniels, A. D.; Farkas, Ö.; Foresman, J. B.; Ortiz, J. V.; Cioslowski, J.; Fox, D. J. *Gaussian 09*, Revision A.1; Gaussian, Inc.: Wallingford, CT, 2009.
(43) *Cerius2*, version 3.0; MSI: Cambridge, U.K.
(44) Our work. Results by Li et al. display slightly shifted values for $(CO)_2Fe(NO)_2$ in THF.
(45) Hedberg, L.; Hedberg, K.; Satija, S. K.; Swanson, B. I. *Inorg. Chem.* **1985**, *24*, 2766.
(46) Chen, H.-W.; Lin, C.-W.; Chen, C.-C.; Yang, L.-B.; Chiang, M.-H.; Liaw, W.-F. *Inorg. Chem.* **2005**, *44*, 3226.
(47) Davies, S. C.; Evans, D. J.; Hughes, D. L.; Konkol, M.; Richards, R. L.; Sanders, J. R.; Sobota, P. *Dalton Trans.* **2002**, 2473.
(48) Chiang, C.-Y.; Lee, J.; Dalrymple, C.; Sarahan, M. C.; Reibenspies, J. H.; Darensbourg, M. Y. *Inorg. Chem.* **2005**, *44*, 9007.